Oxygen Dissociation at Pt Steps

P. Gambardella,[1] Ž. Šljivančanin,[2] B. Hammer,[2] M. Blanc,[1] K. Kuhnke,[1,3] and K. Kern[1,3]

[1]*Institut de Physique Expérimentale, Ecole Polytechnique Fédérale de Lausanne, CH-1015 Lausanne, Switzerland*
[2]*Institute of Physics and Astronomy, University of Aarhus, Ny Munkegade, DK-8000 Aarhus, Denmark*
[3]*Max-Planck-Institut für Festkörperforschung, Heisenbergstrasse 1, D-70569 Stuttgart, Germany*
(Received 14 April 2000; revised manuscript received 22 January 2001; published 12 July 2001)

Using scanning tunneling microscopy, thermal energy atom scattering, and density functional theory we have characterized O_2 dissociation on Pt(111) stepped surfaces at the atomic scale. The most reactive site is at the top of the Pt steps. In both the molecular precursor state (MPS) and the transition state (TS), the O_2 has its axis aligned parallel to the step edge. Controlled step decoration with Ag monatomic chains was used to locally tune the reactivity of Pt step sites. The enhanced reactivity at the Pt step sites is not caused by a decrease of the local dissociation barriers from the MPS but is related to a stabilization of both the MPS and TS.

The behavior of molecules in the proximity of surface defects such as kinks and steps is a central issue in understanding chemisorption processes on catalytic surfaces [1,2]. Recently, specific studies of the step reactivity revealed that steps can determine the overall surface chemistry to a very large extent. Monatomic steps have been shown to completely dominate the dissociation of N_2 and NO on Ru(0001) [2,3] and H_2 on Si(001) [4]. Enhanced step reactivity is generally attributed to a local decrease of the dissociation barriers in the vicinity of step sites related to the reduced coordination of the substrate edge atoms. Density-functional theory (DFT) calculations for the above-mentioned systems [3,4] support this view by showing that the bond-breaking activation barriers with respect to the molecular precursors along the dissociation path are 0.5-1.0 eV lower at edge sites compared to terrace sites. Here, by presenting a detailed analysis of O_2 dissociation on Pt stepped surfaces, we show that surface reaction systems exist for which step sites are most reactive without, however, being associated with the smallest energy barriers.

Because of its relevance in many oxidation reactions that involve Pt as a catalyst, such as that of CO, the adsorption of O_2 on Pt(111) has been extensively studied as a model for dissociative chemisorption. Dissociation of low energy O_2 molecules proceeds by sequential population of physisorbed and chemisorbed precursor states [5–9]. Three chemisorbed molecular states have been identified on Pt stepped surfaces by thermal desorption spectroscopy, electron-energy-loss spectroscopy, and scanning tunneling microscopy (STM) [8,10,11], corresponding to a fcc- and a bridge-bonded terrace species, and a bridge-bonded step species [8]. Steps on Pt(111) are known to bind oxygen molecules and atoms more strongly than terrace sites [5,10–12], and to lead to an increase in oxygen dissociative adsorption with respect to terraces [5,10].

Here, by using a combined experimental and theoretical approach, we demonstrate that O_2 molecules dissociate from a molecular precursor on the upper side of the Pt step edges. The O adatoms resulting from dissociation are found aligned along the Pt step edges, at least two lattice constants apart. Experimentally, the dissociation is strongly favored at step sites which is consistent with our calculations which show a considerable stabilization of the dissociation transition state at step sites. Decoration of the Pt steps by Ag monatomic chains results in a reduction of the measured local reactivity of Pt step sites and, likewise, the calculations show a destabilization of the transition state by the Ag decoration. Since the stability of the molecular precursor state is also affected by the presence of steps and the decoration of these by Ag, the local dissociation energy barrier is—contrary to what might be expected—found to be comparable for Pt terrace and step sites and *smaller* for Ag-decorated Pt step sites. Our results therefore indicate that the enhanced reactivity of Pt step sites originates from steering or lifetime effects associated with the rather stable molecular precursor state at the Pt steps.

Two vicinal surfaces were employed in this paper: Pt[9(111) × (111)] and Pt[8(111) × (100)]. Both surfaces have (111) terraces that are, on average, nine and eight atomic rows wide, separated by {111} and {100} monatomic steps, respectively. Low-temperature STM was used to determine the oxygen dissociation and adsorption sites on Pt[9(111) × (111)], while thermal energy atom scattering (TEAS) was used to control Ag deposition and to measure the relative O_2 dissociation rate for different Ag coverages. The STM images were acquired at 77 K after dosing oxygen at different sample temperatures; typical tunneling parameters were 0.2–6 nA tunneling current and 5–200 mV voltage bias. The experiments were performed with a home-built low-temperature UHV-STM and a triple-axis He spectrometer. The Pt samples were cleaned by sputter-anneal cycles; both surfaces show a remarkable regular distribution of terraces, as evidenced by STM and TEAS diffraction spectra [13]. Oxygen was dosed by backfilling the UHV chambers

at pressures in the 10^{-7}–10^{-6} mbar range. The base pressure was 2×10^{-10} mbar or better.

Figure 1(a) shows the Pt[9(111) $\times$ (111)] surface after exposure to 1.9 L O_2 at 350 K. At this temperature the O atoms resulting from dissociation are highly mobile and occupy the most favored adsorption sites. These are the near-edge fcc sites, in agreement with the results of Feibelman *et al.* [12]. The step sites are completely saturated with a 2×1 periodic structure, whereas very few O atoms can be seen on the terraces, implying sequential site filling. To pinpoint the actual O_2 dissociation sites on a Pt stepped surface we have lowered the adsorption temperature to 140 K. At this temperature the O_2 molecular precursor is highly mobile and its lifetime short: adsorption either results in dissociation or in O_2 desorption [8,10,11]. Since below 160 K the mobility of O atoms on Pt(111) is inhibited [14], the spatial distribution of the dissociated O atoms allows us to identify the active sites in the dissociation process. Figure 1(c) shows the distribution of the O atoms after dosing the Pt[9(111) $\times$ (111)] surface at 140 K with 1.1 L O_2. Ag monatomic chains deposited at 400 K, prior to O_2 dosing, partially decorate the Pt steps. We observe that O_2 dissociation is largely promoted at the step edges, where clean Pt step sites appear to be more reactive with respect to Ag-decorated ones, whereas only a minority of O atoms can be found on the terraces [15]. Since very few O atoms are observed on the lower side of the Pt steps, we conclude that the bond-breaking process involves only the Pt atoms that are situated at the upper step edges. Both O atoms resulting from dissociation occupy near-edge fcc sites, indicating that the O−O bond is stretched in the [1$\bar{1}$0] direction, parallel to the steps. This observation is consistent with a previous STM study by Stipe *et al.* [8] which shows that the O_2 molecules bind in the bridge position at the upper edge of Pt{111} steps with the interatomic axis parallel to the step.

Step decoration can be employed as a means to vary the reactivity of the step sites in a local and controllable way. Ag deposition at 400 K leads to a regular row-by-row growth of Ag chains along the Pt steps which can be precisely monitored by TEAS [13]. We show in Fig. 1(b) that Ag does not physically block the Pt step sites that are active in the dissociation process [16]. Independently from the presence of Ag, oxygen atoms are always found to occupy preferably near-edge fcc sites (with respect to Pt only). To probe the relative variation of the oxygen dissociative sticking coefficient s_0 due to Ag step decoration, we have measured the decay of the TEAS intensity reflected from the sample due to O adsorption on Pt[9(111) $\times$ (111)] and Pt[8(111) $\times$ (100)]. s_0 represents the initial sticking coefficient and it is therefore a measure of the reactivity of step sites. In the limit of low O coverage, the slope of the TEAS curves is proportional to s_0 [17]. Figure 2 shows the variations of s_0 relative to the clean Pt surfaces for different coverages of Ag monatomic wires. The ratio $s_{0\text{-Ag/Pt}}/s_{0\text{-Pt}}$ decreases linearly with the Ag coverage up to complete decoration of the Pt steps by a single chain of Ag atoms. From then on $s_{0\text{-Ag/Pt}}/s_{0\text{-Pt}}$ varies slowly until it drops abruptly as the first Ag monolayer is completed. The data measured by TEAS are in good agreement with the STM data reported in Figs. 1(a) and 1(b): decoration of the steps with one monatomic Ag row yields a tenfold decrease in the reactivity of the steps. The initial linear variation with Ag coverage (see inset in Fig. 2) implies
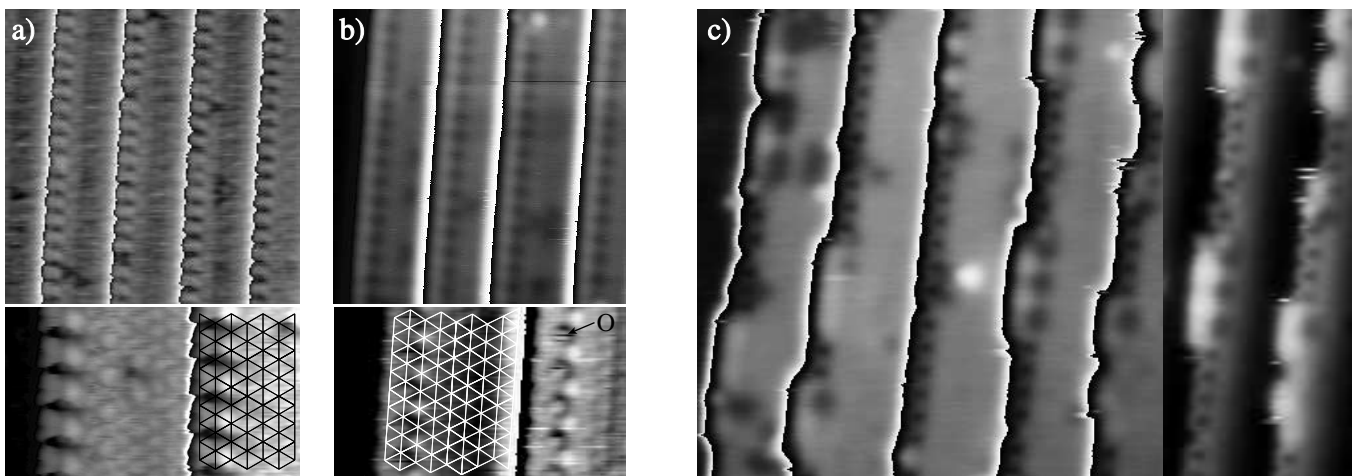

FIG. 1. (a) Top panel: STM image of Pt[9(111) $\times$ (111)] after exposure to 1.9 L (Langmuir) O_2 at 350 K. The O atoms are imaged as black depressions; bottom panel: close-up of the O-saturated Pt steps. (b) Top panel: STM image of one row Ag/Pt[9(111) $\times$ (111)] after exposure to 19 L O_2 at 350 K. Notice that O saturation of the step sites requires 10 times more O_2 compared to (a); bottom panel: O atoms behind the Ag row are imaged dark with a small bump in the middle. (c) Left panel: O atoms following dissociation at 140 K on a partially Ag-decorated surface. As in (a) and (b) the gray scale has been redistributed on each terrace for better contrast; the step-down direction is from right to left. In the right panel we show the right-hand side of the same image without any processing to evidence the Ag monatomic chains at the step edges. These are recognizable because of their larger apparent height with respect to Pt [13].

that the dissociation rate is proportional to the probability of finding an Ag-free region of the step edges. The data presented in Figs. 1 and 2 indicate that Ag locally modifies the reactivity of the Pt edge atoms, an effect that is limited to the Pt atoms in direct contact with Ag. Adsorption along the step atoms does not depend markedly on the total Ag coverage beyond one monatomic chain: the slow $s_{0\text{-Ag/Pt}}/s_{0\text{-Pt}}$ decrease that we observe in Fig. 2 until monolayer completion can be explained by taking into account a reduced O_2 exposure due to the fraction of O_2 molecules that do not stick on the growing Ag layer [18].

To support the above analysis we have performed plane wave, ultrasoft pseudopotential-based DFT calculations for the oxygen molecular precursor and transition states on flat and stepped Pt surfaces. Repeated slabs of four Pt(111), twelve Pt(211), or sixteen Pt(221) layers are used to model adsorption at (111) terraces, {100}, and {111} steps, respectively. The DFT equilibrium lattice constant of 4.02 Å is used self-consistently with the generalized gradient approximation (GGA) based revised Perdew-Burke-Ernzerhof exchange-correlation functional (GGA-RPBE) [19] and non–self-consistently with the original GGA-type Perdew-Wang exchange-correlation functional (GGA-PW91) [20] exchange-correlation functionals. Substrate relaxation effects have been included, and surface Brillouin-zone integrations are done using 6×4 **k**-points. Transition states are determined by performing geometry optimization calculations with the O–O distance fixed at values from 1.8 to 2.2 Å (and larger when necessary), with increments of 0.2 Å. Test calculations show that the molecule precursor state geometry on Pt(221) and its potential energy are very close to the results on Pt(211); we therefore limit here the discussion to Pt(111) and Pt(211). In the following, we will focus on the GGA-RPBE values as this functional provides the more accurate O_2 molecular binding energy, $E_b^{\text{RPBE}} = 5.51$ eV versus $E_b^{\text{PW91}} = 5.84$, compared

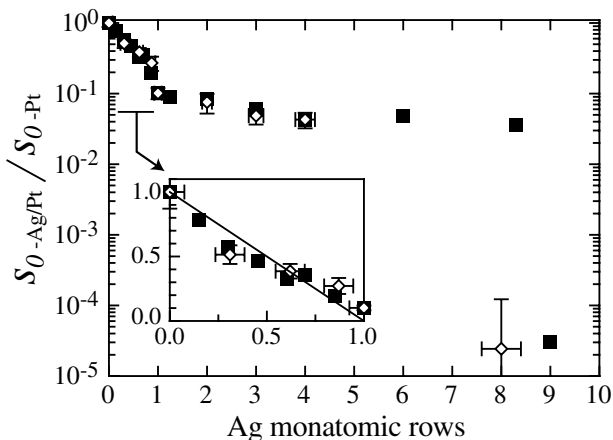to the experimental result, $E_b^{\text{exp}} = 5.23$ eV [19]. The GGA-PW91 values are, however, included in Fig. 3 for consistency with the existing literature. The difference between the GGA-RPBE and GGA-PW91 results illustrates the uncertainties in the DFT method.

Figure 3 (top panel) shows the molecular precursor state (MPS) geometries for Pt(111), Pt(211), and Ag/Pt(211) and the calculated local molecular chemisorption potential energy minima, E_{MPS}, and transition state (TS) potential energies, E_{TS} (bottom panel). The energy values are given with respect to gas phase O_2. Our GGA-PW91 results are in agreement with Ref. [7], which reports on the MPS of O_2 at Pt(111). Reaction geometries other than those depicted in Fig. 3, e.g., with O_2 tilted perpendicular to the steps or out from the surface plane, were found to be unfavorable.

The molecular precursor chemisorption potential energy minima vary substantially from terrace to step sites: -0.1 eV on Pt(111), -0.9 eV on Pt(211) steps, and -0.3 eV on Ag-decorated steps. The transition state energies follow the E_{MPS} trend. As a consequence, the local dissociation energy barriers $E_a = E_{\text{TS}} - E_{\text{MPS}}$ vary less than the stability of the individual precursor and transition states: $E_a = 0.9$, 0.9, and 0.6 eV on Pt(111), Pt(211), and Ag-decorated steps, respectively. Our results can be analyzed in terms of the d-band model for chemisorption and reaction at transition and noble metals

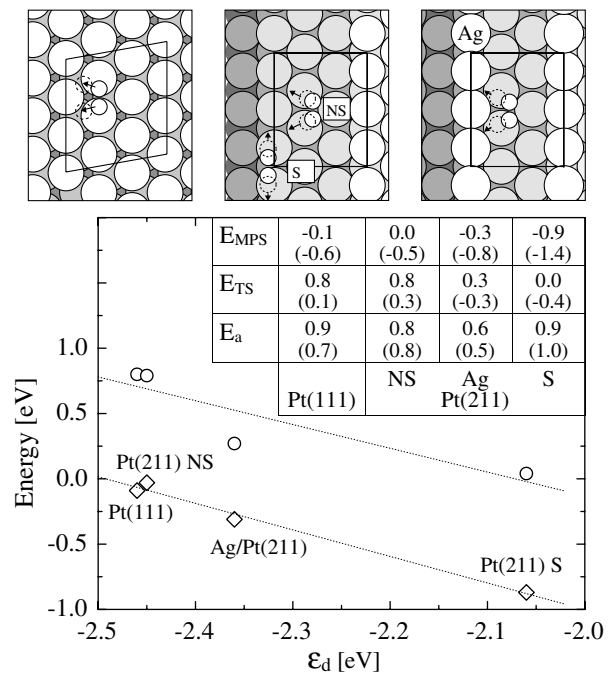|		Pt(111)		Pt(211)	
			NS	Ag	S
E_{MPS}	-0.1 (-0.6)	0.0 (-0.5)	-0.3 (-0.8)	-0.9 (-1.4)
E_{TS}	0.8 (0.1)	0.8 (0.3)	0.3 (-0.3)	0.0 (-0.4)
E_a	0.9 (0.7)	0.8 (0.8)	0.6 (0.5)	0.9 (1.0)

FIG. 3. Top: molecular precursor states and transition states (solid and dotted circles, respectively) on Pt(111), Pt(211) step (S) and "near step" (NS) sites, Ag/Pt(211) (Ag). Bottom: molecular precursor state potential energies (◇) and transition state energies (○) as functions of the d-electron centers. The GGA-RPBE (GGA-PW91) results are presented in the table shown in the figure.

FIG. 2. Variation of the O_2 dissociation rate with respect to the Ag-free step value for Pt[9(111) $\times$ (111)] (■) and Pt[8(111) $\times$ (100)] (◇) at 400 K.

[21]. Compared to the reference situation at Pt(111), the Pt $5d$-band centers shift to higher energies at the Ag-decorated Pt step and to yet higher energies at the clean Pt step sites. This reflects that terrace Pt is highly coordinated with neighboring Pt atoms, while step Pt is lower coordinated. Smaller coordination leads to band narrowing and, through local charge neutrality, to upshifts in the Pt $5d$-band position. As metal d bands contribute significantly to the chemisorption bonds, the net result is that, as shown in Fig. 3, the potential energy of the molecular precursor and transition states correlates with the Pt $5d$-band center.

Figure 3 shows that the molecular precursor state and transition state are stabilized by similar amounts for a given shift of the d-band center. As a consequence, E_a becomes rather independent of the d-band center. The smaller E_a calculated for Ag-decorated Pt steps therefore appears to be caused by other effects—possibly from direct O_2-Ag interaction.

In previous studies [2–4], enhanced dissociation at step sites was shown to depend on a local lowering of the activation barriers for the local molecular adsorption species. For O_2 on Pt, however, we find that these barrier heights and the dissociation rates are anticorrelated, in particular for the Ag-decorated and clean Pt step cases. Only when considering the energy barrier with respect to gas-phase O_2 rather than to molecular chemisorbed O_2 (i.e., considering E_{TS} rather than E_a) the enhanced reactivity of the Pt steps becomes apparent from the DFT results (cf. Fig. 3). The use of E_{TS} rather than E_a in interpreting the experimental results is, however, highly relevant. We shall consider the two extreme situations: (i) O_2 in thermal equilibrium with the surface and (ii) O_2 behaving as a hot precursor. In the first situation, E_a must be compared to the desorption energy barrier, $E_d = -E_{MPS}$, because this barrier determines the lifetime of the molecular precursor. The branching ratio of the two competing events, dissociation and desorption, becomes exponentially dependent on the difference, $E_a - E_d = E_{TS}$, whereby the importance of E_{TS} for the local reactivity becomes apparent. In the other extreme situation, where the O_2 acts as a hot precursor, the local stability of the MPS provides us with information on the potential energy surface (PES) for the precursor. This PES shows strong steering forces [22] from the Pt terrace sites towards the Pt step sites and less so towards the Ag-decorated Pt step sites. As a hot precursor, the O_2 has kinetic energy up to $E_{kin,0} - E_{MPS}$, where $E_{kin,0}$ is the kinetic energy upon impact, available for surmounting the local energy barrier, E_a. For this situation, $E_{kin,0} - E_{MPS} - E_a = E_{kin,0} - E_{TS}$ becomes a measure of the local excess kinetic energy of the dissociating precursor. Again, it is seen that E_{TS} is the key parameter for the local reactivity. The O_2/Pt system constitutes, to our knowledge, the first case where the enhanced reactivity of step sites cannot be associated with a lowering of the activation barrier, E_a. The exact behavior of the O_2, whether in thermal equilibrium or acting as a hot precursor, is unknown, but experimental evidence indicates the first scenario as the more likely [6,11].

[1] G. A. Somorjai, *Introduction to Surface Chemistry and Catalysis* (Wiley, New York, 1994).

[2] T. Zambelli *et al.,* Science **273**, 1688 (1996).

[3] S. Dahl *et al.,* Phys. Rev. Lett. **83**, 1814 (1999); B. Hammer, Phys. Rev. Lett. **83**, 3681 (1999).

[4] P. Kratzer *et al.,* Phys. Rev. Lett. **81**, 5596 (1998).

[5] J. L. Gland, Surf. Sci. **93**, 487 (1980).

[6] C. T. Campbell *et al.,* Surf. Sci. **107**, 220 (1981); A. C. Luntz, M. D. Williams, and D. S. Bethune, J. Chem. Phys. **89**, 4381 (1988); A. C. Luntz, J. Grimblot, and D. E. Fowler, Phys. Rev. B **39**, 12 903 (1989); P. D. Nolan *et al.,* J. Chem. Phys. **111**, 3696 (1999).

[7] A. Eichler and J. Hafner, Phys. Rev. Lett. **79**, 4481 (1997).

[8] B. C. Stipe *et al.,* Phys. Rev. Lett. **78**, 4410 (1997).

[9] T. Zambelli *et al.,* Nature (London) **495**, 495 (1997).

[10] A. Winkler *et al.,* Surf. Sci. **201**, 419 (1988).

[11] M. R. McClellan, F. R. McFeely, and J. L. Gland, Surf. Sci. **123**, 188 (1983); H. Wang *et al.,* Surf. Sci. **372**, 267 (1997); A. T. Gee and B. E. Hayden, J. Chem. Phys. **113**, 10 333 (2000).

[12] P. J. Feibelman, S. Esch, and T. Michely, Phys. Rev. Lett. **77**, 2257 (1996).

[13] P. Gambardella *et al.,* Phys. Rev. B **61**, 2254 (2000).

[14] J. Wintterlin, R. Schuster, and G. Ertl, Phys. Rev. Lett. **77**, 123 (1996).

[15] Uneven O coverage on different terraces is attributed to the increased dissociation probability in the vicinity of chemisorbed O atoms (Ref. [9]).

[16] Direct dissociation on Ag steps is considered negligible. Figure 2 shows that O adsorption on a stepped Ag monolayer is small compared to Pt.

[17] B. Poelsema and G. Comsa, *Scattering of Thermal Atoms* (Springer, Berlin, 1989).

[18] F. Buatier de Mongeot, U. Valbusa, and M. Rocca, Surf. Sci. **339**, 291 (1995).

[19] B. Hammer, L. B. Hansen, and J. K. Nørskov, Phys. Rev. B **59**, 7413 (1999).

[20] J. P. Perdew *et al.,* Phys. Rev. B **46**, 6671 (1992).

[21] B. Hammer and J. K. Nørskov, Adv. Catal. **45**, 71 (2000).

[22] A. Gross, S. Wilke, and M. Scheffler, Phys. Rev. Lett. **75**, 2718 (1995).